Chemistry of Iron with Dipicolinic Acid. 1. Mononuclear Complexes of Iron(II) or Iron(III)

P. Lainé, A. Gourdon,* and J.-P. Launay

Molecular Electronics Group, CEMES, CNRS UP8011, BP4347, 29 Rue J. Marvig, 31055 Toulouse Cedex, France

Received January 27, 1995[⊗]

The synthesis, characterization, and properties of dipicolinic acid ($dipicH_2$) derivatives are described. Neutralization of hot aqueous concentrated solutions of $dipicH_2$ showed successive gelifications–liquefaction processes. Isolation of crystalline-phase $[(dipicH)(dipicH_2)]Na\cdot 3H_2O$ (**1**) revealed an intricate network of interactions among the acid, the sodium cation, and water molecules. $[(dipic)Fe^{II}(OH_2)_3]$ (**2**) was prepared in nearly quantitative yield by reaction of $dipic^{2-}$ with an excess of ammonium iron(II) sulfate hexahydrate. **2** reacts with bases $(cation^+)OH^-$ to give $[(dipic)_2Fe^{II}](cation)_2$ in high yields (**3**: cation = $NProp_4^+$). $[(dipic)_2Fe^{II}]^{2-}$ was solvatochromic, due to interactions between the dipic oxygen lone pairs and solvents. Air or bromine water oxidation of **3** yielded quantitatively the iron(III) complexes $[(dipic)_2Fe^{III}](cation)$ (**4**: cation = Na^+). The crystal structures of **1**–**4** have been determined. Comparison of the geometries of **3** and **4** showed that the iron–nitrogen bond lengths are insensitive to iron oxidation states whereas the iron-oxygen distances decrease by 0.15 Å upon iron oxidation. This allowed the calculation of the intervalence band energy in dipic mixed-valence systems. **1** crystallized in the triclinic space group $P\bar{1}$ with cell constants $a = 6.882(1)$ Å, $b = 11.125(2)$Å, $c = 11.171(2)$ Å, $\alpha = 82.65(4)°$, $\beta = 82.13(4)°$, $\gamma = 87.38(6)°$, $V = 844(3)$ Å^3, and $Z = 2$. **2** was found in the monoclinic space group $P2_1/c$ with $a = 12.410(4)$ Å, $b = 9.314(4)$ Å, $c = 8.746(3)$ Å, $\beta = 101.44(4)°$, $V = 990(1)$ Å^3, and $Z = 4$. **3**·$7.25H_2O$ occurred in the monoclinic space group $P2_1/c$ with $a = 15.320(9)$ Å, $b = 33.83(2)$ Å, $c = 17.24(1)$ Å, $\beta = 91.55(4)°$, $V = 8932(9)$ Å^3, and with $Z = 8$. **4**·H_2O crystallized in the monoclinic space group Cc with $a = 14.95(1)$ Å, $b = 12.45(3)$ Å, $c = 8.663(5)$ Å, $\beta = 92.99(4)°$, $V = 609(4)$ Å^3, and $Z = 4$.

Introduction

The complexation of metal ions by 2,6-pyridinedicarboxylic acid (dipicolinic acid, $dipicH_2$) has been extensively studied. This stems mainly from its ability to form stable chelates,[1] with various coordination modes such as bidentate,[2] meridian,[3] or bridging.[4] Other interesting properties are its biological activity,[5] its ability to stabilize unusual oxidation states,[6] and its usefulness in analytical chemistry[7] such as chemical analysis of iron at low concentration[7a] (down to 4 ppm), in corrosion inhibition[8] and in decontamination of nuclear reactors;[9] the iron complexes have also been used as electron carriers in model biological sytems,[10] as well as specific molecular tools in DNA cleavage.[11] Finally, iron complexes of dipicolinate are involved in one of the greatest challenges of modern homogeneous catalysis, namely iron-induced activation of dioxygen and hydrogen peroxide.[12]

As part of a study of electron transfer through "molecular wires", we were interested in preparing and measuring the electron transfer properties of dinuclear iron complexes linked by conjugated ethynylated dipic subunits close to those described by Kankare *et al.*[13] This study required a deeper understanding of the chemistry of iron complexes containing dipicolinic acid and led us to entirely re-examine this subject.

In the literature, only four iron dipic complexes have been described: $[(dipic)_2Fe^{II}](cation)_2$ (solution studies,[7,14] syntheses with cation = Na^+, Ba^{2+} [10a,12g,14a]), $[(dipic)_2Fe^{III}]^-$ (thermodynamic study,[14c] synthesis and X-ray structure for cation =

[⊗] Abstract published in *Advance ACS Abstracts,* September 1, 1995.

(1) (a) Erikson, T. E.; Grenthe, I.; Puigdomenech, I. *Inorg. Chim. Acta* **1987**, *126*, 131. (b) Ducommun, Y.; Helm, L.; Laurenczy, G.; Merbach, A. *Inorg. Chim. Acta* **1989**, *158*, 3.
(2) (a) Ventur, D.; Wieghardt, K.; Weiss, J. Z. *Anorg. Allg. Chem.* **1985**, *524*, 40. (b) Zhou, X. Y.; Kostic, N. M. *Inorg. Chem.* **1988**, *27*, 4402. (c) Herring, A. M.; Henling, L.; Labinger, J. A.; Bercaw, J. E. *Inorg. Chem.* **1991**, *30*, 851.
(3) (a) Fürst, W.; Gouzerh, P.; Jeannin, Y. *J. Coord. Chem.* **1979**, *8*, 237. (b) Drew, M. G. B; Fowles, G. W. A.; Matthews, R. W.; Walton, R. A. *J. Am. Chem. Soc.* **1969**, *91*, 7769. (c) Drew, M. G. B; Matthews, R. W.; Walton, R. A. *J. Chem. Soc. A* **1970**, 1405.
(4) (a) Nardin, G.; Randaccio, L.; Bonomo, R. P.; Rizzarelli, E. *J. Chem. Soc., Dalton Trans* **1980**, 369. (b) Sengupta, S. K.; Shani, S. K.; Kapoor, R. N. *Polyhedron* **1983**, *2*, 317.
(5) (a) Bailey, G. F.; Karp, S.; Sacks, T. E. *J. Bacteriol.* **1965**, *89*, 984. (b) Setlow, B.; Setlow, P. *Appl. Environ. Microbiol.* **1993**, *59*, 640. (b) Waterbury, L. D.; Serrato, C.; Martinez, G. R. *Proc. West Pharmac. Soc.* **1989**, *32*, 9.
(6) Hoof, D. L.; Tisley, D. G.; Walton, R. A. *J. Chem. Soc., Dalton Trans.* **1973**, 200 and references therein.
(7) (a) Morimoto, I.; Tanaka, S. *Anal. Chem.* **1963**, *35*, 1234. (b) Kanay, Y. *Analyst (London)* **1990**, *115*, 809.
(8) (a) Every, R. L.; Riggs, O. L., Jr. *Mater. Protect.* **1964**, *3*, 46. (b) Campanella, L.; De Angelis, G. *Ann. Univ. Ferrara Ser.* **1970**, *5*, 565.
(9) Pope, C. G.; Matijevic, E.; Patel, R. C. *J. Colloid Interface Sci.* **1981**, *80*, 874.
(10) (a) Mauk, A. G.; Coyle, C. L.; Bordignon, E.; Gray, H. B. *J. Am. Chem. Soc.* **1979**, *101*, 5054. (b) Harrington, P. C.; Wilkins, R. G. *J. Inorg. Biochem.* **1980**, *12*, 107. (c) Mauk, A. G.; Bordignon, E.; Gray, H. B. *J. Am. Chem. Soc.* **1982**, *104*, 7654.
(11) Groves, J. T.; Kady, I. O. *Inorg. Chem.* **1993**, *32*, 3868.
(12) (a) Sheu, C.; Sawyer, D. T. *J. Am. Chem. Soc.* **1990**, *112*, 8212. (b) Sugimoto, H.; Tung, H.-C.; Sawyer, D. T. *J. Am. Chem. Soc.* **1988**, *110*, 2465. (c) Dalton, H. *Adv. Appl. Microbiol.* **1980**, *26*, 71. (d) Ericson, A.; Hedman, B.; Hodgson, K. O.; Green, J.; Dalton, H.; Bentsen, J. G.; Beer, S.; Lippard, S. J. *J. Am. Chem Soc.* **1988**, *110*, 2330. (e) Fox, B. G.; Surerus, K. K.; Munck, E.; Lipscomb, J. D. *J. Biol. Chem.* **1988**, *263*, 10553. (f) Sheu, C.; Sobkowiak, A.; Jeon, S.; Sawyer, D. T. *J. Am. Chem. Soc.* **1990**, *112*, 879. (g) Cofré, P.; Richert, S. A.; Sobkowiak, A.; Sawyer, D. T. *Inorg. Chem.* **1990**, *29*, 2645. (h) Tung, H.-C.; Kang, C.; Sawyer, D. T. *J. Am. Chem. Soc.* **1992**, *114*, 3445. (i) Balavoine, G.; Barton, D. H. R.; Gref, A.; Lellouche, I. *Tetrahedron* **1992**, *48*, 1883.
(13) (a) Takalo, H.; Kankare, J.; Hänninen, E. *Acta Chem. Scand.* **1988**, *B42*, 448. (b) Takalo, H.; Kankare, J. *Acta Chem. Scand.* **1987**, *B41*, 219. (c) Hänninen, E.; Takalo, H.; Kankare, J. *Acta Chem. Scand.* **1988**, *B42*, 614.

0020-1669/95/1334-5129$09.00/0

$H_5O_2^+$ [15]), $[(dipicH)_2Fe^{II}]$ (existence mentioned or postulated[12f,12g,16]), and a dinuclear complex $[(dipic)Fe^{III}(OH_2)(\mu\text{-}OH)]_2$ (synthesis, properties, and structure[17]). We found the chemistry of iron with dipicolinic acid to be much more complex than expected, particularly in the solid state. Thus the present series of papers reports several new aspects, of potential interest for the synthesis of elaborate compounds.

In paper 1, we report mononuclear complexes of iron(II) and iron(III) containing only the dipic ligand. We obtained the $[(dipic)Fe^{II}(OH_2)_3]$ complex (**2**), which can be used as a precursor for the synthesis of mixed-ligand species. We have also specified and compared the structures of $[(dipic)_2Fe^{II}]^{2-}$ (**3**) and $[(dipic)_2Fe^{III}]^-$ (**4**).

In paper 2, we describe several surprising structures obtained in the solid state, in which the $[(dipic)_2Fe^{II}]^{2-}$ unit shows its ability to act as a ligand by complexation through the free oxygens of the carboxylate groups.

Paper 3 is devoted to two new heptacoordinated structures of iron(II).

Finally, paper 4 deals with the complexes of iron(III) with one dipic ligand and other various ligands (chloride, water, acetylacetonate, *o*-phenanthroline, etc.).

Experimental Section

All manipulations were performed under argon atmosphere with carefully degassed solvents. 2,6-Pyridinedicarboxylic acid ($dipicH_2$) and ammonium iron(II) sulfate hexahydrate (Mohr's salt) were used as received (Aldrich). FTIR spectra were run as KBr pellets on a Perkin-Elmer 1725 X and UV−vis on a Shimadzu UV-PC 3101.

Mössbauer spectra were obtained on a constant-acceleration conventional spectrometer with a 25 mCi source of ^{57}Co (Rh matrix). Throughout the papers of this series, isomer shift values (δ) are given with respect to metallic iron at room temperature. The absorber was a sample of 160−200 mg of microcrystalline powder enclosed in a 2 cm diameter cylindrical plastic holder, the size of which had been determined to optimize the absorption. The samples were prepared in a glovebox. Variable-temperature spectra were obtained in the 300−4.2 K range, by using an MD 306 Oxford cryostat, the thermal scanning being monitored by an Oxford ITC4 servocontrol device (±0.1 K accuracy). A least-squares computer program[18] was used to fit the Mössbauer parameters and determine their standard deviations of statistical origin (given in parentheses).

Variable-temperature magnetic susceptibility data were obtained with a Quantum Design MPMS SQUID susceptometer. The samples (10 mg) were ground with agar in a glovebox. Diamagnetic corrections were applied using Pascal's constants.[19] Least-squares fittings were carried out with the program STEPT.[20]

Preparation of [(dipicH)(dipicH$_2$)]Na. A suspension of $dipicH_2$ (1.5 g, 8.98 mmol) in water (15 mL) was neutralized by dropwise addition of 5 M aqueous NaOH. When the acid was dissolved, the solution was heated to the boiling point and concentrated to 15 mL, and the pH was adjusted to 3.5 by addition of concentrated HCl. Slow cooling afforded white crystals of $[(dipicH)(dipicH_2)]Na{\cdot}3H_2O$ (yield 22.5%). FTIR (KBr, cm^{-1}): 3477 vs, 3089, 2538 (ν_{sym} OH); 1730, 1703 s (ν_{asym} free COOH); 1672, 1660 (ν_{asym} coordinated COOH); 1588 (ν_{asym} COO^-). Anal. Calcd for $C_{14}H_{15}N_2NaO_{11}$: C, 40.99; H, 3.68; N, 6.83. Found: C, 41.02; H, 3.70; N, 6.80.

Preparation of [(dipic)Fe^{II}(OH$_2$)$_3$]. A degassed aqueous (100 mL) solution of $dipicH_2$ (8.55 g, 51.16 mmol) at 100 °C under argon was neutralized by dropwise addition of 5 M NaOH. An excess of Mohr's salt (23 g, 58.65 mmol) was then added, and the mixture was stirred for 0.5 h at 100 °C, left to cool to room temperature, and then left at 4 °C for 1 week. Filtration of the mixture gave orange leaflets; rapid washing with ethanol, diethyl ether, and drying by suction filtration under argon yielded 13.76 g of $[(dipic)Fe^{II}(OH_2)_3]$ (98% vs $dipicH_2$). The crystals can be stored in the cold under argon. Anal. Calcd for $C_7H_9NFeO_7$: C, 30.57; H, 3.28; N, 5.08; Fe, 20.31. Found: C, 30.52; H, 3.21; N, 5.08; Fe, 20.29. FTIR (KBr, cm^{-1}): 3255 vs (ν_{sym} OH); 1651, 1610, 1587 s (ν_{asym} COO); 1471, 1427 (ν_{sym} COO). UV−vis in H_2O, pH 7.0 (λ_{max}, nm ($10^{-2}\epsilon$, $dm^3\ mol^{-1}\ cm^{-1}$)): 446 (6.21), 270 (48), 266 (49.5), 195 (370).

Preparation of [(dipic)$_2$Fe^{II}](cation)$_2$. Method a (Cation = Na). A degassed aqueous (160 mL) solution of $dipicH_2$ (15.0 g, 89.75 mmol) at 70 °C under argon was neutralized by dropwise addition of 6 M NaOH (final volume around 190 mL). Mohr's salt (17.3 g, 44.12 mmol) was then added, the mixture was stirred 2 h at 70 °C, left to cool to room temperature, and then left at 4 °C for 1 week. The dark red crystals were then rapidly filtered off under argon, washed with acetone and diethyl ether, and dried under argon. Concentration of the mother liquors gave an another crop. Total yield: 18.7 g (90.5% vs Mohr's salt). The crystals can be stored in the cold under argon. They rapidly lose their water of crystallization. Anal. Calcd for $[(dipic)_2Fe^{II}]Na_2{\cdot}2H_2O$ ($C_{14}H_{10}N_2FeO_{10}Na_2$): C, 35.92; H, 2.15; N, 5.98; Fe, 11.93; Na, 9.82. Found: C, 35.87; H, 2.15; N, 5.97; Fe, 11.80; Na, 9.69. FTIR (KBr, cm^{-1}): 1625 s (ν_{asym} COO); 1427 (ν_{sym} COO). UV−vis (cation = Na^+) in H_2O, pH 6.5 (λ_{max}, nm (ϵ, $dm^3\ mol^{-1}\ cm^{-1}$)): 482 (1350) (MLCT); 269 (9500) ($n\pi^*$).

Method b1 (Cation = TPA, N(C$_3$H$_7$)$_4$). To a suspension of $[(dipic)Fe^{II}(OH_2)_3]$ (159 mg, 0.578 mmol) in acetonitrile (40 mL) was added dropwise over 2 h a solution of 5×10^{-2} M tetrapropylammonium hydroxide in methanol (11 mL, 0.55 mmol). The excess $[(dipic)Fe^{II}(OH_2)_3]$ and iron hydroxide were removed by filtration. Addition of diethyl ether to the filtrate gave a precipitate which was washed with ether and recrystallized from acetone, yielding 208 mg (yield 95% vs TPA) of very hygroscopic dihydrate. Anal. Calcd for $C_{38}H_{66}N_4FeO_{10}$: C, 57.42; H, 8.37; N, 7.05; Fe, 7.02. Found: C, 57.16; H, 8.36; N, 6.97; Fe, 7.17.

Method b2 (Cation = TPA). To an aqueous solution (75 mL) of $[(dipic)Fe^{II}(OH_2)_3]$ (149.7 mg, 0.512 mmol) was added dropwise an aqueous 5×10^{-2} solution of tetrapropylammonium hydroxide (10.5 mL, 0.525 mmol). After 0.5 h of stirring, the solvent was removed under vacuum and the product was extracted with dichloromethane, reprecipitated with diethyl ether, washed with ether, and recrystallized from acetone or acetonitrile. The tetrahydrate is hygroscopic. Yield: 185 mg, 85% vs TPA. Anal. Calcd for $C_{38}H_{70}N_4FeO_{12}$: C, 54.94; H, 8.49; N, 6.74; Fe, 6.72. Found: C, 54.89; H, 8.37; N, 6.78; Fe, 6.63.

Synthesis of [(dipic)$_2$Fe^{III}](cation). Slow air oxidation or addition of bromine to an aqueous solution of $[(dipic)_2Fe^{II}](cation)_2$ gave quantitatively $[(dipic)_2Fe^{III}](cation)$. The product could then be recrystallized from acidic water or ethanol.

(a) Cation = Na$^+$. Anal. Calcd for $[(dipic)_2Fe^{III}]Na{\cdot}2H_2O$ ($C_{14}H_{10}N_2FeO_{10}Na$): C, 37.78; H, 2.26; N, 6.29; Fe, 12.55; Na, 5.16. Found: C, 37.58; H, 2.24; N, 6.29; Fe, 12.91; Na, 5.20. FTIR (KBr, cm^{-1}): 1674, 1632 (ν_{asym} COO); 1431 (ν_{asym} COO).

(b) Cation = NH$_4^+$. Anal. Calcd for $[(dipic)_2Fe^{III}](NH_4)$ ($C_{14}H_{10}N_3FeO_8$): C, 41.61; H, 2.49; N, 10.40; Fe, 13.82. Found: C, 41.52; H, 2.46; N, 10.34; Fe, 13.41. FTIR (KBr, cm^{-1}): 3162 (ν NH); 1652, 1592 (ν_{asym} COO); 1447 (ν_{sym} COO).

(c) Cation = N(C$_4$H$_9$)$_4^+$. Anal. Calcd for $C_{30}H_{42}N_3FeO_8$: C, 57.33; H, 6.73; N, 6.68; Fe, 8.88. Found: C, 57.38; H, 6.62; N, 6.69; Fe, 8.78. FTIR (KBr, cm^{-1}): 3083, 2962, 2936, 2875 (ν C−H in $N(C_4H_9)_4^+$); 1672, 1596 (ν_{asym} COO); 1472, 1423 (ν_{sym} COO). UV−vis (cation = NH_4^+) in H_2O, pH 6.5 (λ_{max}, nm (ϵ, $dm^3\ mol^{-1}\ cm^{-1}$)): 675 (2.3) (br, d-d); 478 (5.5) (d-d); 271 (12 300) (sh, $n\pi^*$); 254 (13 800) ($n\pi^*$); 195 (80 000) ($\pi\pi^*$).

(14) (a) Bertram, H.; Wieghardt, K. *Inorg. Chem.* **1979**, *18*, 1799. (b) Hartkamp, H. Z. *Anal. Chem.* **1962**, *190*, 66. (c) Anderegg, G. *Helv. Chim. Acta* **1960**, *43*, 1530.
(15) (a) Hseu, J. F.; Chen, J. J.; Wei, H. H.; Cheng, M. C.; Wang, Y.; Yao, Y. D. *Inorg. Chim. Acta* **1991**, *184*, 1. (b) Marsh, R. E. *Acta Crystallogr.* **1993**, *C49*, 643. (c) Cousson, A.; Nectoux, F. *Acta Crystallogr.* **1992**, *C48*, 1354.
(16) D'Ascenzo, G.; Marino A.; Sabbatini, M.; Bica, T. *Thermochim. Acta* **1978**, *25*, 325.
(17) Thich, J. A.; Ou, C. C.; Powers, D.; Wasiliou, B.; Mastropaolo, D.; Potenza, J. A.; Schugar, H. J. *J. Am. Chem. Soc.* **1976**, *98*, 1425.
(18) Varret, F. *Proceedings of the International Conference on Mössbauer Effect Applications*, Jaipur, India, 1981; Indian National Science Academy: New Delhi, 1982.
(19) Carlin, R. L. *Magnetochemistry*; Springer-Verlag: Berlin Heidelberg, 1986; p 3.
(20) Chandler, J. P. Program 66, Quantum Chemistry Program Exchange, Indiana University, 1973.

Table 1. Crystallographic Data for $[(dipicH)(dipicH_2)]Na\cdot 3H_2O$ (**1**), $[(dipic)Fe^{II}(OH_2)_3]$ (**2**), $[(dipic)_2Fe^{II}][N(C_3H_7)_4]_2\cdot 7.25H_2O$ (**3**), and $[(dipic)_2Fe^{III}]Na\cdot 2H_2O$ (**4**)

	1	**2**	**3**	**4**
formula	$C_{14}H_{15}N_2NaO_{11}$	$C_7H_9NFeO_7$	$C_{38}H_{76.5}N_4FeO_{23.25}$	$C_{14}H_{10}N_2FeNaO_{10}$
fw	410.27	275.02	1648.17	445.08
space group	$P\bar{1}$ (No. 2)	$P2_1/c$ (No. 14)	$P2_1/c$ (No. 14)	Cc (No. 9)
a, Å	6.882(1)	12.410(4)	15.320(9)	14.95(1)
b, Å	11.125(2)	9.314(4)	33.83(2)	12.45(3)
c, Å	11.171(2)	8.746(3)	17.24(1)	8.663(3)
α, deg	82.65(4)	90	90	90
β, deg	82.13(4)	101.44(4)	91.55(4)	92.99(4)
γ, deg	87.38(6)	90	90	90
V, Å^3	844(3)	990(1)	8932(9)	1609(4)
Z	2	4	8	4
T, °C	21	21	21	21
μ(Mo Kα), cm^{-1}	1.53	15.39	3.92	10.20
ϱ_{calcd}, g cm^{-3}	1.61	1.843	1.22	1.84
R^a	0.031	0.036	0.057	0.022
$R_w{}^b$	0.031	0.043	0.057	0.023

$^a R = \sum||F_o| - |F_c||/\sum|F_o|$. $^b R_w = [\sum w(|F_o| - |F_c|)^2/\sum w|F_o|^2]^{1/2}$.

X-ray Crystallography. Details of the crystal data and a summary of intensity data collection parameters are presented in Table 1.

Unit cell parameters were obtained by centering 25 reflections having 2θ values between 22 and 30°. Data were collected on an Enraf-Nonius CAD-4 diffractometer using graphite-monochromated Mo Kα radiation (0.710 69 Å) and $\omega-2\theta$ scans. For each structure, the data were corrected for Lorentz and polarization effects. Data with intensities less than $n\sigma(I)$ were excluded from the refinements. Scattering factors were from ref 21 and were corrected for anomalous dispersion. When necessary, absorption corrections were carried out using the DIFABS[22] or PSISCAN[23] methods and the secondary extinction parameter was calculated according to ref 24.

For $[(dipic)_2Fe^{II}](TPA)_2$, the asymmetric unit contains 2 complexes, 4 tetrapropylammonium counterions, and 7.25 water molecules. The propyl chains of one of the cations are disordered over two positions. Soft constraints were then applied to the carbon atoms of these chains with a free overall occupation factor. This factor converged to 0.5, a value to which it was then fixed in further refinements. The terminal methyl hydrogen atoms were located on Fourier maps and refined with soft constraints. One of the water molecules [O(800)] which had a low peak height was refined with a fixed isotropic temperature factor of 0.06 Å^2 and a variable occupation factor which converged to $^1/_4$, a value to which it was then fixed in the next steps. Its hydrogen atoms were not localized on Fourier maps. The hydrogen atoms of the pyridine rings and of the propyl chains were positioned geometrically, their positions being recalculated after each refinement cycle.

In the final stages of the refinements, to each reflection was assigned a weight calculated from a Chebyshev series with three coefficients.[25] The final refinements were done with a block approximation of the matrix. The structures were solved using SHELXS,[26] and all further calculations were performed using the CRYSTALS software package.[27] Drawings were obtained using ORTEP.[28] For clarity, the thermal vibration ellipsoids are drawn with a probability level of 20% and the hydrogen atoms are drawn with an artificial B of 1.02 Å^2. Selected atomic coordinates, bond distances, and bond angles are presented in the tables.

Results and Discussion

The dipicolinate anion with its two carboxylate groups in ortho positions with respect to the pyridine nitrogen is potentially tridentate. Obviously, the reactivity of the ligand for complexation depends on its degree of protonation, as it can exist as $dipic^{2-}$, $dipicH^-$, or $dipicH_2$. The acidity constants of dipicolinic acid have been determined by several groups;[29] in the following, we have used the values reported by Wieghardt[2a] coming from the pioneering work of Anderegg,[29a] i.e. $pK_{a_1} = 2.10$ and $pK_{a_2} = 4.68$. The preparation of dipic complexes requires the deprotonation of dipicolinic acid. However, it turned out that this is not a simple process, and some unusual observations are reported below.

Preliminary Study of $dipicH_2$ Neutralization. Addition of a concentrated aqueous solution of sodium hydroxide (5 mol L^{-1}) to a concentrated boiling suspension of $dipicH_2$ (0.5 mol L^{-1}) causes a spectacular sequence of gelifications (during which the solution thickens considerably) and redissolutions in narrow pH intervals. Thus the thickening of the solution occurs successively at pH 3.30, 4.85, and 5.30. Between these values, the gel liquefies progressively, and slightly above pH 5.3, the solution is completely clear.

This observation has not been fully explained; nevertheless, it is known that dipic is strongly aggregated in aqueous acidic solutions.[30] Thus the formation of these gels could correspond to three different intricate networks of strong H bonds and electrostatic interactions at these pH values and Na^+ concentrations. An example is given by the structure of the sodium salt $[(dipicH)(dipicH_2)]Na\cdot 3H_2O$. It is obtained by cooling a pH 3.5 solution, this solution having been prepared by neutralizing $dipicH_2$ with an excess of base and then acidifying progressively, as described in the Experimental Section.

The X-ray structure of $[(dipicH)(dipicH_2)]Na\cdot 3H_2O$ (**1**) is shown in Figure 1. Selected bond lengths and angles are given in Table 3. The sodium cation is surrounded by three water molecules, one oxygen atom from a $dipicH_2$, and two oxygens and one nitrogen from a $dipicH^-$, at distances ranging from 2.275(2) to 2.584(2) Å. The two dipic molecules are nearly planar, with maximum deviations less than 0.1 Å, except for the CO_2 groups O(11)−C(1)−O(12) and O(171)−C(17)−

(21) *International Tables for X-ray Crystallography*; The Kynoch Press: Birmingham, England, 1974.
(22) Walker, N.; Stuart, D. *Acta Crystallogr.* **1979**, *B35*, 2387.
(23) North, A. C. T.; Phillips, D. C.; Mathews, F. S. *Acta Crystallogr.* **1968**, *A24*, 351.
(24) Larson, A. C. *Crystallographic Computing*; Munksgaard: Copenhagen, 1970; p 22.
(25) (a) Prince, E. *Mathematical Techniques in Crystallography;* Springer-Verlag: Berlin, 1982. (b) Carruthers, J. R.; Watkin, D. J. *Acta Crystallogr.* **1979**, *A35*, 698.
(26) Sheldrick, G. M. SHELXS86. Program for the solution of crystal structures. University of Göttingen, Germany, 1985.
(27) Watkin, D. J.; Carruthers J. R.; Betteridge, P. W. CRYSTALS: An Advanced Crystallographic Computer Program. Chemical Crystallographic Laboratory, Oxford University, 1990.
(28) Johnson, C. K. ORTEPII. Report ORNL-5138; Oak Ridge National Laboratory: Oak Ridge, 1976.
(29) (a) Anderegg, G. *Helv. Chim. Acta* **1960**, *43*, 414. (b) Sillen, L. G.; Martell, A. E. *Stability Constants of Metal Ions*; The Chemical Society: London, 1964. (c) Petifaux, C.; Fournaise, R. *Bull. Soc. Chim. Fr.* **1972**, *3*, 914. (d) Cariati, F.; Naldini, L.; Panzanelli, A.; Demartin, F.; Manassero, M. *Inorg. Chim. Acta* **1983**, *69*, 117.
(30) Peral, F. *J. Mol. Struct.* **1992**, *266*, 373.

Table 2. Selected Atomic Coordinates and Equivalent Isotropic Thermal Parameters (Å^2) for [(dipicH)(dipicH$_2$)]Na·3H$_2$O (**1**)

atom	*x/a*	*y/b*	*z/c*	*U*(iso)[a]
Na(1)	0.1971(1)	−0.20184(7)	−0.05437(7)	0.0351
N(1)	0.2631(3)	0.2141(1)	−0.2853(1)	0.0280
C(1)	0.2110(3)	0.0040(2)	−0.2937(2)	0.0322
C(2)	0.2649(3)	0.1231(2)	−0.3579(2)	0.0297
C(3)	0.3105(4)	0.1367(2)	−0.4824(2)	0.0377
C(4)	0.3574(4)	0.2494(2)	−0.5358(2)	0.0404
C(5)	0.3529(4)	0.3441(2)	−0.4630(2)	0.0362
C(6)	0.3050(3)	0.3233(2)	−0.3388(2)	0.0288
C(7)	0.2974(3)	0.4281(2)	−0.2599(2)	0.0342
O(11)	0.1839(3)	−0.0120(1)	−0.1848(1)	0.0394
O(12)	0.1938(3)	−0.0800(1)	−0.3679(1)	0.0417
O(71)	0.2589(3)	0.4039(1)	−0.1466(1)	0.0419
O(72)	0.3265(3)	0.5288(1)	−0.3096(2)	0.0469
N(11)	0.2379(3)	−0.2677(2)	0.1537(2)	0.0307
C(11)	0.2236(3)	−0.4744(2)	0.1019(2)	0.0348
C(12)	0.2150(3)	−0.3828(2)	0.1952(2)	0.0314
C(13)	0.1863(4)	−0.4182(2)	0.3176(2)	0.0389
C(14)	0.1837(4)	−0.3320(2)	0.4007(2)	0.0408
C(15)	0.2123(4)	−0.2132(2)	0.3588(2)	0.0374
C(16)	0.2376(3)	−0.1857(2)	0.2350(2)	0.0316
C(17)	0.2643(4)	−0.0576(2)	0.1852(2)	0.0378
O(111)	0.2400(3)	−0.4319(1)	−0.0081(1)	0.0394
O(112)	0.2156(3)	−0.5826(1)	0.1356(2)	0.0447
O(171)	0.2610(3)	−0.0408(1)	0.0693(1)	0.0424
O(172)	0.2842(3)	0.0221(1)	0.2517(2)	0.0483
O(100)	−0.1596(3)	−0.1792(2)	0.0166(2)	0.0444
O(200)	0.1007(3)	−0.2794(2)	−0.2419(2)	0.0500
O(300)	0.5039(3)	−0.2257(2)	−0.1570(2)	0.0619
H(12)	0.158(4)	−0.149(3)	−0.322(3)	0.0700

[a] Equivalent isotropic *U*(iso) defined as one-third of the trace of the orthogonalized tensor.

O(172) which show angles of 6.6 and 7.6° with respect to the pyridine mean planes. These mean planes are nearly parallel (7.6°), and the Na^+ ion is located between these two planes at 0.77 Å from the dipicH$_2$ plane and at 0.56 Å from the dipicH$^-$ plane. The acidic H atoms are involved in strong hydrogen bonds as shown by the distances following (Å): O(200)−H(12) = 1.67(3) and O(200)−O(12) = 2.593(2); O(111)−H(71) = 1.41(3) and O(111)−O(71) = 2.470(2); O(100)−H(171) = 1.69(3) and O(100)−O(171) = 2.659(2). Other weaker hydrogen bonds involve water molecules and carboxylic oxygen atoms (Å): O(72)−H(202) = 1.77(4) and O(200)−O(72) = 2.676(3); O(172)−H(301) = 2.02(3) and O(172)−O(300) = 2.810(3).

This 3-dimensional network illustrates one of the possible arrangements of electrostatic interactions and hydrogen bonds among dipicH$_2$, dipicH$^-$, dipic^{2-}, Na^+, and water at the origin of the gelification processes encountered during neutralization of concentrated dipicH$_2$ solutions.

Synthesis, Structure, and Properties of [(dipic)Fe^{II}(OH$_2$)$_3$] (2). Our first aim was the preparation of a precursor of the type [(dipic)Fe^{II}L$_3$] with labile ligands L, allowing later the synthesis of dinuclear mixed-valence complexes such as [(dipic)-Fe^{II}(dipic−R−dipic)Fe^{III}(dipic)]$^{3-}$ by reaction of this precursor with a bridging ligand bearing terminal dipic groups. Although the 1:1 complex of iron(II) and dipic was mentioned in solution studies,[29b] it had never been isolated and was sometimes considered unstable.[16]

[(dipic)Fe^{II}(OH$_2$)$_3$] can be prepared nearly quantitatively by reaction of an excess of ammonium iron(II) sulfate hexahydrate (Mohr's salt) with dipicH$_2$ at a pH such that the two acid functions are neutralized. The orange product is very soluble in water and DMSO, soluble in DMF, slightly soluble in methanol and ethanol, and insoluble in most other solvents. Figure 2 shows the structure of the complex. Selected bond lengths and angles are given in Table 5. The iron environment is a distorted octahedron. The dipic ligand is planar, with deviations smaller than 0.1 Å, except for O(11), involved in a strong intermolecular hydrogen bond, and lies 0.17 Å away from the mean plane. As observed in all other dipic complexes, the metal−N distance [2.086(2) Å] is short with respect to the metal−oxygen distances [2.157(1) and 2.189(1) Å]. This point will be discussed later in the text. Due to steric repulsions between the dipic ligand and the axial water molecules, the axial bonds are not perpendicular to the dipic mean plane, with O(130)−Fe(1)−N(1) = 92.40(6)°, O(110)−Fe(1)−N(1) = 95.59(6)°, and O(110)−Fe(1)−O(130) = 168.67(6)°.

It must be noticed that the Fe(1)−O(130) is significantly longer than Fe(1)−O(110) and Fe(1)−O(120) [respectively 2.213(1), 2.093(1), and 2.086(1) Å]. This is correlated to differences in the bonding geometries of the water molecules. The molecules H(116)−O(110)−H(117) and H(126)−O(120)−H(127) are bound in such a way that their C_2 axis goes through Fe(1) (case 1 in Figure 3). Thus, the bond with the metal simultaneously involves the two oxygen lone pairs. In contrast, the water molecule H(136)−O(130)−H(137) is bound in such a way (case 2) that only one lone pair is involved in the bonding, which weakens it with respect to the previous case. Consequently, for the two former molecules, the sums of the three angles around the oxygen atoms are nearly 360° [357.5° around O(110) and 350.2° around O(120)] whereas this sum is 315.2° around O(130).

The reasons for these different bonding geometries in the solid state are not clear so far. In particular, it is difficult to explain why the chemically equivalent H(136)−O(130)−H(137) and H(117)−O(110)−H(116) water molecules are bound differently to iron. This may be due to different patterns of hydrogen bonding. These water molecules are indeed involved in a net of intermolecular hydrogen bonds as shown by the following distances (Å): O(11)−H(117) = 1.75(4) and O(11)−O(110) = 2.694(2); O(12)−H(116) = 1.89(5) and O(12)−O(110) = 2.747(2); O(71)−H(136) = 2.03(5) and O(71)−O(130) = 2.788 (2); O(72)−H(127) = 1.82(5) and O(72)−O(120) = 2.754(2); O(72)−H(137) = 1.87(5) and O(72)−O(130) = 2.699(2). Oddly enough, the water molecule least involved in hydrogen bonding, H(136)−O(130)−H(137), is also the more weakly bound to the metal atom.

The results of Mössbauer spectroscopy are in good agreement with these crystallographic results. Simulation of the spectra obtained at various temperatures gives the isomer shifts and quadrupolar splittings, respectively δ and ΔE_Q (mm s^{-1}): at 293 K, 1.137 and 3.891; at 221 K, 1.182 and 4.021; at 149 K, 1.225 and 4.093; at 80 K, 1.257 and 4.138. These values of δ indicate that, above 80 K, the iron atom is high-spin Fe(II). The high ΔE_Q shows an important axial distortion which can correspond either to the long Fe(1)−O(130) bond or to the axial compression along the pseudo C_2 axis N(1)−Fe(1)−O(120). The rapid variation of ΔE_Q as a function of temperature indicates that the first excited state is high in energy.

Magnetic susceptibility shows a magnetic moment of 5.40 μ_B at 300 K, which confirms that the Fe(II) is high spin at room temperature. This value decreases steadily on cooling down to 40 K, probably due to temperature-independent paramagnetism as observed in other distorted Fe(II) complexes. It drops more rapidly between 40 and 5 K, to a final value of 4.61 μ_B, which could be due either to zero-field splitting or to weak intermolecular interactions (antiferromagnetic coupling) through the hydrogen bond network.

Synthesis, Structure, and Solvatochromism of [(dipic)$_2$Fe^{II}]-(cation)$_2$ (Cation = Na^+, NProp$_4^+$). According to the

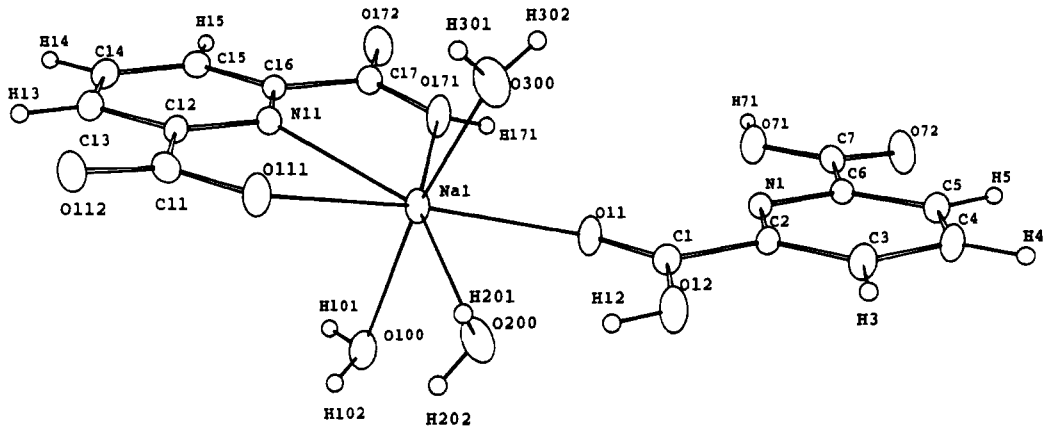

Figure 1. Structure of the cation environment in **1**.

Table 3. Selected Bond Distances (Å) and Angles for [(dipicH)(dipicH$_2$)]Na·3H$_2$O (**1**)

Na(1)–O(11)	2.478(2)	Na(1)–O(100)	2.481(2)
Na(1)–N(11)	2.433(2)	Na(1)–O(200)	2.506(2)
Na(1)–O(111)	2.584(2)	Na(1)–O(300)	2.275(2)
Na(1)–O(171)	2.434(2)		
N(1)–C(2)	1.342(3)	N(11)–C(12)	1.337(3)
N(1)–C(6)	1.337(3)	N(11)–C(16)	1.336(3)
C(1)–C(2)	1.495(3)	C(11)–C(12)	1.505(3)
C(1)–O(11)	1.207(3)	C(11)–O(111)	1.275(3)
C(1)–O(12)	1.314(3)	C(11)–O(112)	1.235(3)
C(2)–C(3)	1.381(3)	C(12)–C(13)	1.383(3)
C(3)–C(4)	1.380(3)	C(13)–C(14)	1.382(3)
C(4)–C(5)	1.375(3)	C(14)–C(15)	1.382(3)
C(5)–C(6)	1.386(3)	C(15)–C(16)	1.383(3)
C(6)–C(7)	1.509(3)	C(16)–C(17)	1.500(3)
C(7)–O(71)	1.268(3)	C(17)–O(171)	1.297(3)
C(7)–O(72)	1.224(3)	C(17)–O(172)	1.223(3)
N(11)–Na(1)–O(11)	139.16(6)	O(200)–Na(1)–N(11)	141.00(7)
O(111)–Na(1)–O(11)	155.88(6)	O(200)–Na(1)–O(111)	78.98(6)
O(111)–Na(1)–N(11)	64.05(6)	O(200)–Na(1)–O(171)	152.90(7)
O(171)–Na(1)–O(11)	73.80(6)	O(200)–Na(1)–O(100)	86.49(7)
O(171)–Na(1)–N(11)	65.44(6)	O(300)–Na(1)–O(11)	84.29(7)
O(171)–Na(1)–O(111)	128.08(6)	O(300)–Na(1)–N(11)	103.65(8)
O(100)–Na(1)–O(11)	90.55(6)	O(300)–Na(1)–O(111)	82.41(7)
O(100)–Na(1)–N(11)	87.13(6)	O(300)–Na(1)–O(171)	98.48(8)
O(100)–Na(1)–O(111)	98.57(6)	O(300)–Na(1)–O(100)	168.28(9)
O(100)–Na(1)–O(171)	90.12(7)	O(300)–Na(1)–O(200)	82.23(8)
O(200)–Na(1)–O(11)	79.35(6)		
C(6)–N(1)–C(2)	117.0(2)	C(16)–N(11)–C(12)	117.7(2)
O(11)–C(1)–C(2)	122.9(2)	O(111)–C(11)–C(12)	115.8(2)
O(12)–C(1)–C(2)	113.2(2)	O(112)–C(11)–C(12)	119.2(2)
O(12)–C(1)–O(11)	123.9(2)	O(112)–C(11)–O(111)	125.0(2)
C(1)–C(2)–N(1)	114.8(2)	C(11)–C(12)–N(11)	116.8(2)
C(3)–C(2)–N(1)	123.5(2)	C(13)–C(12)–N(11)	122.6(2)
C(3)–C(2)–C(1)	121.7(2)	C(13)–C(12)–C(11)	120.6(2)
C(4)–C(3)–C(2)	118.6(2)	C(14)–C(13)–C(12)	119.1(2)
C(5)–C(4)–C(3)	118.6(2)	C(15)–C(14)–C(13)	118.9(2)
C(6)–C(5)–C(4)	119.3(2)	C(16)–C(15)–C(14)	118.2(2)
C(5)–C(6)–N(1)	122.9(2)	C(15)–C(16)–N(11)	123.6(2)
C(7)–C(6)–N(1)	118.3(2)	C(17)–C(16)–N(11)	116.2(2)
C(7)–C(6)–C(5)	118.9(2)	C(17)–C(16)–C(15)	120.2(2)
O(71)–C(7)–C(6)	116.5(2)	O(171)–C(17)–C(16)	114.4(2)
O(72)–C(7)–C(6)	118.1(2)	O(172)–C(17)–C(16)	120.9(2)
O(72)–C(7)–O(71)	125.5(2)	O(172)–C(17)–O(171)	124.7(2)

literature,[14b] the synthesis of [(dipic)$_2$Fe^{II}](cat)$_2$ is similar to the one for other [(dipic)$_2$M]$^{n+}$ complexes: after neutralization of dipicH$_2$ in water, addition of FeCl$_2$ and cation exchange generally precipitate the product. This method is well adapted to alkaline and alkaline-earth cations (method a in the following), but the very good solubility in water of the alkylammonium salts precludes the preparation of the corresponding salts by cation exchange in water. We have prepared these latter derivatives in organic solvents in one step by treating [(dipic)Fe^{II}(OH$_2$)$_3$] with base (cation)OH:

$$2\,\text{cation}^+ + 2\text{OH}^- + 2[(\text{dipic})\text{Fe}^{II}(\text{OH}_2)_3] \rightarrow [(\text{dipic})_2\text{Fe}^{II}](\text{cation})_2\ (\text{soluble}) + [(\text{HO})_2\text{Fe}(\text{OH}_2)_4]\ (\text{precipitate})$$

The synthesis can be done in a solvent in which [(dipic)Fe^{II}(OH$_2$)$_3$] is insoluble (method b1) or soluble (method b2) and provides high yields of pure products. It can be extended to alkaline and alkaline-earth cations, by reaction of the corresponding base in water. When the cation is tetrapropylammonium or tetrabutylammonium, the compounds are very soluble in all usual polar solvents, but surprisingly not in acetone.

Interestingly, these compounds are very solvatochromic. The main absorption in the visible region comes from a metal-to-ligand charge transfer (MLCT) band, the position of which changes from 565 nm in DMF to 460 nm in dilute acetic acid solution (see Table 6). We have searched for a correlation between these wavelengths and pertinent parameters such as the dielectric constant ϵ, the donor number[31] DN, and the acceptor number[32] AN of the solvents. Only the last parameter gave a significant correlation: it appears clearly in Figure 4 that λ_{MLCT} decreases linearly with AN. This behavior is similar to that of [(CN)$_2$Fe^{II}(phen)$_2$] (phen = *o*-phenanthroline), for which an interaction between the nitrogen of the CN ligand (Lewis base) and the solvent (Lewis acid) is assumed.[33] By analogy, in the present case, the most likely interaction involves the free oxygen of the carboxylate groups playing the role of Lewis base. Incidentally, this explains why acetone, which has the lowest AN, is a poor solvent for these complexes.

The X-ray structure of the tetrapropylammonium salt has been solved. Selected bond lengths and angles are given in Table 8. The asymmetric unit contains two [(dipic)$_2$Fe^{II}]$^{2-}$ anions, four cations, and 7.25 crystallization water molecules. Figure 5 shows an ORTEP drawing of the two cations with the numbering scheme. Within a complex, the ligands are nearly perpendicular, with angles between mean planes of 96.0 and 92.7°. This trans meridional geometry is similar to that observed for other transition metals such as Cr^{III},[3a] Ru^{II},[2a] or Fe^{III}.[15b,15c] The dipic ligands are nearly planar (maximum deviation 0.05 Å) except for the carboxylic groups O(171)–C(17)–O(172) and O(311)–C(31)–O(312). These groups are slightly off the pyridine mean planes with deviations of 8.3 and 7.0°, respectively. The carboxylic and water oxygen atoms are linked through a complex network of hydrogen bonds as shown by the distances in Table 9.

(31) Gutman, V.; Wychera, E. *Inorg. Nucl. Chem. Lett.* **1966**, *2*, 257.
(32) Mayer, U. *Pure Appl. Chem.* **1979**, *51*, 1697.
(33) Soukup, R. W.; Schmid, R. *J. Chem. Educ.* **1985**, *62*, 459. Micheau, J.-C.; Lavabre, D.; Levy, G. *Actual. Chim.* **1988**, 241.

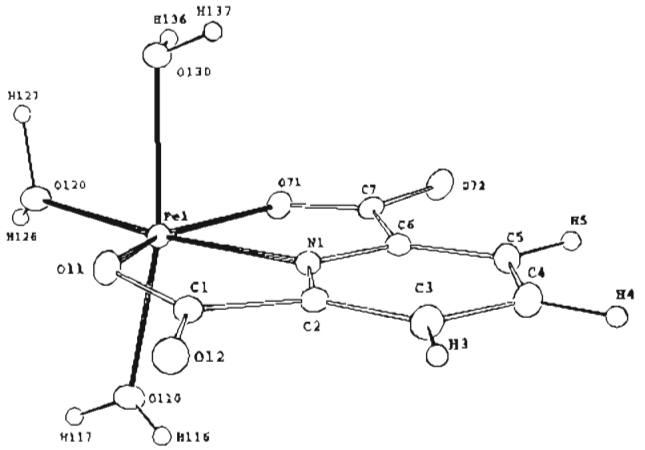

Figure 2. ORTEP diagram for $[(dipic)Fe^{II}(OH_2)_3]$ (**2**).

Table 4. Selected Atomic Coordinates and Equivalent Isotropic Thermal Parameters ($Å^2$) for $[(dipic)Fe^{II}(OH_2)_3]$ (**2**)

atom	*x/a*	*y/b*	*z/c*	*U*(iso)[a]
Fe(1)	0.28852(2)	0.08265(3)	−0.00806(3)	0.0210
N(1)	0.2234(1)	−0.1214(2)	0.0121(2)	0.0210
C(1)	0.1034(2)	0.0040(2)	0.1458(2)	0.0225
C(2)	0.1385(1)	−0.1364(2)	0.0822(2)	0.0213
C(3)	0.0931(2)	−0.2697(2)	0.0994(2)	0.0281
C(4)	0.1398(2)	−0.3888(2)	0.0436(3)	0.0307
C(5)	0.2309(2)	−0.3729(2)	−0.0245(2)	0.0273
C(6)	0.2691(2)	−0.2355(2)	−0.0414(2)	0.0222
C(7)	0.3665(2)	−0.1969(2)	−0.1124(2)	0.0243
O(11)	0.1670(1)	0.1102(2)	0.1349(2)	0.0270
O(12)	0.0217(1)	0.0076(2)	0.2047(2)	0.0292
O(71)	0.3869(1)	−0.0646(2)	−0.1195(2)	0.0282
O(72)	0.4216(1)	−0.2945(2)	−0.1573(2)	0.0326
O(110)	0.1680(1)	0.1462(2)	−0.1987(2)	0.0308
O(120)	0.3733(1)	0.2721(2)	−0.0317(2)	0.0323
O(130)	0.4107(1)	0.0579(2)	0.2119(2)	0.0248

[a] Equivalent isotropic *U*(iso) defined as one-third of the trace of the orthogonalized tensor.

Table 5. Bond Lengths (Å) and Angles (deg) for $[(dipic)Fe^{II}(OH_2)_3]$ (**2**)

Fe(1)−N(1)	2.086(2)	Fe(1)−O(130)	2.213(1)
Fe(1)−O(11)	2.157(1)	C(1)−O(11)	1.280(2)
Fe(1)−O(71)	2.189(1)	C(1)−O(12)	1.225(2)
Fe(1)−O(110)	2.093(1)	C(7)−O(71)	1.262(2)
Fe(1)−O(120)	2.086(2)	C(7)−O(72)	1.247(3)

O(11)−Fe(1)−N(1)	74.47(6)	O(120)−Fe(1)−O(71)	98.56(6)
O(71)−Fe(1)−N(1)	74.12(6)	O(120)−Fe(1)−O(110)	88.66(6)
O(71)−Fe(1)−O(11)	148.03(5)	O(130)−Fe(1)−N(1)	92.40(6)
O(110)−Fe(1)−N(1)	95.59(6)	O(130)−Fe(1)−O(11)	86.89(6)
O(110)−Fe(1)−O(11)	87.52(6)	O(130)−Fe(1)−O(71)	88.59(6)
O(110)−Fe(1)−O(71)	101.31(6)	O(130)−Fe(1)−O(110)	168.67(6)
O(120)−Fe(1)−N(1)	172.12(7)	O(130)−Fe(1)−O(120)	84.38(6)
O(120)−Fe(1)−O(11)	112.43(7)		

The Mössbauer chemical shifts and quadrupolar splittings for the sodium salt are respectively as follows: 1.013 (2.858) mm s^{-1} at 293 K; 1.059 (3.141) mm s^{-1} at 221 K; 1.098 (3.393) mm s^{-1} at 149 K; 1.127 (3.544) mm s^{-1} at 80 K. These chemical shifts are smaller than in $[(dipic)Fe^{II}(OH_2)_3]$, which indicates that the iron is more electron rich in $[(dipic)_2Fe^{II}]^{2-}$ (N_2O_4 environment versus NO_5 in $[(dipic)Fe^{II}(OH_2)_3]$). The relatively high values of quadrupolar splitting reflect the compression of the octahedron along the nitrogen−iron−nitrogen direction.

The magnetic moment 5.35 μ_B at 300 K indicates that the iron is high spin. As for the previous compound, it decreases slowly down to 50 K (5.24 μ_B) and then more rapidly from 50 to 5 K (4.50 μ_B) for the same reasons.

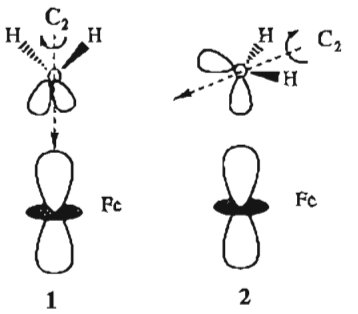

Figure 3. Bonding geometries of water molecules in **2**. Case 1: the sum of Fe−O−H and H−O−H angles is ≈360°. Case 2: the sum of Fe−O−H and H−O−H angles is ≪360°.

Table 6. MLCT Wavelengths (nm) of **3** in Various Solvents[a]

solvent	AN	DN	ϵ	$\lambda_{max,MLCT}$
acetone	12.5	17.0	20.7	565.0
acetonitrile	18.9	14.1	37.5	547.5
CH_2Cl_2	20.4		8.9	543.0
$CHCl_3$	23.1		4.8	538.0
$CH_3CO_2H + H_2O$	52.9		6.2	459.5
DMF	16.0	26.6	36.7	565.5
DMSO	19.3	29.8	46.7	559.0
ethanol	37.1		24.6	516.5
methanol	41.3	19.0	32.7	505.5
nitrobenzene	14.8	4.4	34.8	560.0
nitromethane	20.5	2.7	35.9	532.5
pyridine	14.2	33.1	12.4	566.0
water	54.8	18.0	80.2	485.0

[a] AN is the acceptor number, DN is the donor number, and ϵ is the dielectric constant.

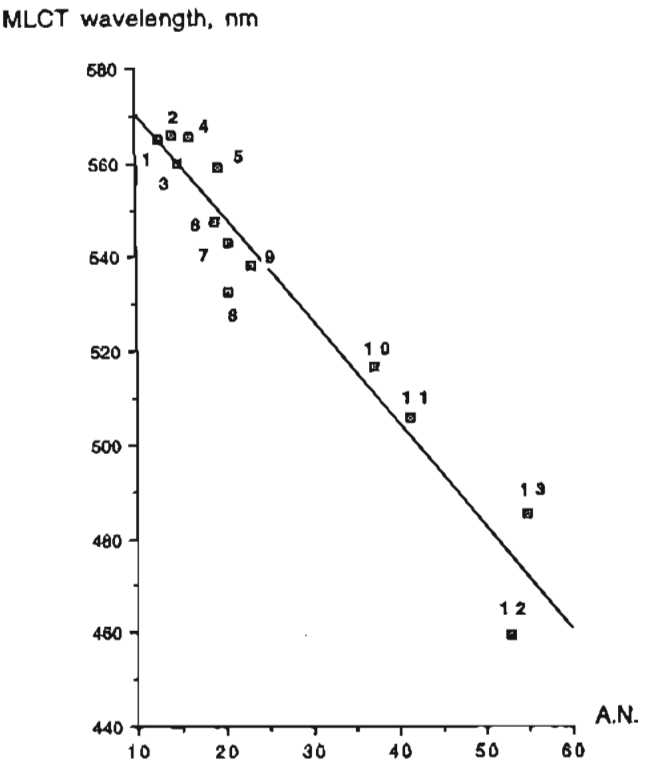

Figure 4. Wavelengths of the MLCT band of $[(dipic)_2Fe^{II}]^{2-}$ vs solvent acceptor numbers (AN): (1) acetone; (2) pyridine; (3) nitrobenzene; (4) dimethylformamide; (5) acetonitrile; (6) dimethyl sulfoxide; (7) dichloromethane; (8) nitromethane; (9) chloroform; (10) ethanol; (11) methanol; (12) dilute acetic acid; (13) water.

Synthesis and Structure of $[(dipic)_2Fe^{III}]$(cation). $[(dipic)_2Fe^{III}]$(cation) can be obtained by slow air oxidation of $[(dipic)_2Fe^{II}]$(cation)$_2$ or oxidation by bromine water and recrystallization from slightly acidic water (pH 5.5) (or from ethanol when the

Table 7. Selected Positional and Equivalent Isotropic Thermal Parameters (Å²) for $[(dipic)_2Fe^{II}][N(C_3H_7)_4]_2 \cdot 7.25H_2O$ (**3**)

atom	*x/a*	*y/b*	*z/c*	*U*(iso)[a]
Fe(1)	0.27960(9)	0.62357(4)	0.02708(8)	0.0563
N(1)	0.2633(4)	0.5640(2)	0.0498(4)	0.0431
C(1)	0.2890(6)	0.5568(3)	−0.0858(5)	0.0574
C(2)	0.2671(5)	0.5378(2)	−0.0072(5)	0.0446
C(3)	0.2524(6)	0.4986(3)	0.0053(5)	0.0571
C(4)	0.2318(6)	0.4861(3)	0.0781(6)	0.0622
C(5)	0.2280(6)	0.5134(3)	0.1380(5)	0.0546
C(6)	0.2444(5)	0.5527(2)	0.1215(5)	0.0469
C(7)	0.2432(5)	0.5857(3)	0.1800(6)	0.0530
O(11)	0.2967(4)	0.5935(2)	−0.0840(3)	0.0674
O(12)	0.2953(4)	0.5344(2)	−0.1412(3)	0.0718
O(71)	0.2586(4)	0.6195(2)	0.1533(3)	0.0632
O(72)	0.2302(4)	0.5775(2)	0.2485(4)	0.0692
N(11)	0.2773(5)	0.6844(2)	0.0144(4)	0.0538
C(11)	0.1237(7)	0.6746(3)	−0.0001(5)	0.0615
C(12)	0.2003(6)	0.7031(3)	0.0044(5)	0.0571
C(13)	0.1974(7)	0.7434(3)	−0.0006(6)	0.0776
C(14)	0.2739(8)	0.7649(3)	0.0041(7)	0.0791
C(15)	0.3517(7)	0.7452(3)	0.0142(6)	0.0700
C(16)	0.3511(6)	0.7046(3)	0.0182(5)	0.0536
C(17)	0.4309(7)	0.6779(3)	0.0260(5)	0.0673
O(111)	0.1432(4)	0.6385(2)	0.0039(4)	0.0662
O(112)	0.0494(4)	0.6883(2)	−0.0058(4)	0.0836
O(171)	0.4132(4)	0.6414(2)	0.0374(4)	0.0664
O(172)	0.5038(5)	0.6925(2)	0.0201(5)	0.0912
Fe(2)	0.27117(8)	0.38661(4)	0.48028(8)	0.0578
N(21)	0.2606(4)	0.4465(2)	0.4626(4)	0.0483
C(21)	0.2655(5)	0.4285(3)	0.3288(6)	0.0522
C(22)	0.2584(5)	0.4608(3)	0.3901(5)	0.0495
C(23)	0.2481(6)	0.5005(3)	0.3766(5)	0.0602
C(24)	0.2389(7)	0.5254(3)	0.4382(7)	0.0729
C(25)	0.2419(6)	0.5108(3)	0.5125(6)	0.0653
C(26)	0.2518(5)	0.4707(3)	0.5228(5)	0.0511
C(27)	0.2582(6)	0.4492(3)	0.6013(6)	0.0566
O(211)	0.2705(4)	0.3938(2)	0.3545(3)	0.0623
O(212)	0.2656(4)	0.4387(2)	0.2597(4)	0.0716
O(271)	0.2660(4)	0.4125(2)	0.5966(3)	0.0607
O(272)	0.2532(5)	0.4698(2)	0.6596(4)	0.0788
N(31)	0.2765(5)	0.3263(2)	0.4998(4)	0.0538
C(31)	0.1221(6)	0.3327(3)	0.5131(5)	0.0542
C(32)	0.2023(6)	0.3067(3)	0.5125(5)	0.0563
C(33)	0.2030(7)	0.2667(3)	0.5239(7)	0.0822
C(34)	0.2844(9)	0.2474(3)	0.5206(9)	0.0939
C(35)	0.3596(7)	0.2679(3)	0.5083(7)	0.0761
C(36)	0.3532(6)	0.3075(3)	0.4983(5)	0.0537
C(37)	0.4270(6)	0.3361(3)	0.4843(5)	0.0519
O(311)	0.1350(4)	0.3677(2)	0.4933(3)	0.0604
O(312)	0.0513(4)	0.3186(2)	0.5310(4)	0.0703
O(371)	0.4077(4)	0.3718(2)	0.4797(4)	0.0638
O(372)	0.5012(4)	0.3212(2)	0.4782(4)	0.0723

[a] Equivalent isotropic *U*(iso) defined as one-third of the trace of the orthogonalized tensor.

cation is aliphatic). $[(dipic)_2Fe^{III}]Na \cdot 2H_2O$ crystallizes in the noncentrosymetric space group *Cc*. The asymmetric unit contains one complex and two water molecules. The geometry of the complex (Figure 6) is very similar to that of the parent Fe^{II} complex. As expected, the Fe−O distances (Table 11) are 0.1−0.15 Å shorter than in the Fe^{II} complex, with distances ranging from 2.000(3) to 2.053(3) Å. On the contrary, the Fe^{III}−N bond is not shorter than in the Fe^{II} complex (Figure 7) with Fe^{III}−N = 2.057(3) Å. In the iron(II) complexes, coordination of the two carboxylate groups induces an important compression of the iron−nitrogen bond. Analogous uncompressed iron(II)−pyridine bond distances are found in the range 2.20−2.30 Å.[34] Oxidation of the metal atom contracts the iron radius by *ca.* 0.15 Å and allows some relaxation of the compression energy by bending the carboxylate groups toward the iron atom. The iron(III)−nitrogen bond distances are then in the normal range, which could be related to the higher

Table 8. Selected Distances (Å) and Angles (deg) for $[(dipic)_2Fe^{II}][N(C_3H_7)_4]_2 \cdot 7.25H_2O$ (**3**)

Fe(1)−N(1)	2.069(6)	Fe(2)−N(21)	2.055(7)
Fe(1)−O(11)	2.190(6)	Fe(2)−O(211)	2.182(6)
Fe(1)−O(71)	2.213(6)	Fe(2)−O(271)	2.191(6)
Fe(1)−N(11)	2.068(7)	Fe(2)−N(31)	2.069(7)
Fe(1)−O(111)	2.176(6)	Fe(2)−O(311)	2.200(6)
Fe(1)−O(171)	2.137(6)	Fe(2)−O(371)	2.151(6)
C(1)−O(11)	1.25(1)	C(21)−O(211)	1.257(9)
C(1)−O(12)	1.23(1)	C(21)−O(212)	1.24(1)
C(7)−O(71)	1.258(9)	C(27)−O(271)	1.25(1)
C(7)−O(72)	1.234(9)	C(27)−O(272)	1.23(1)
C(11)−O(111)	1.26(1)	C(31)−O(311)	1.25(1)
C(11)−O(112)	1.23(1)	C(31)−O(312)	1.231(9)
C(17)−O(171)	1.28(1)	C(37)−O(371)	1.246(9)
C(17)−O(172)	1.23(1)	C(37)−O(372)	1.251(9)
O(11)−Fe(1)−N(1)	74.4(2)	O(111)−Fe(1)−O(71)	91.8(2)
O(71)−Fe(1)−N(1)	74.4(2)	O(111)−Fe(1)−N(11)	74.7(3)
O(71)−Fe(1)−O(11)	148.7(2)	O(171)−Fe(1)−N(1)	112.3(2)
N(11)−Fe(1)−N(1)	170.6(3)	O(171)−Fe(1)−O(11)	93.8(2)
N(11)−Fe(1)−O(11)	111.8(3)	O(171)−Fe(1)−O(71)	95.8(2)
N(11)−Fe(1)−O(71)	99.4(2)	O(171)−Fe(1)−N(11)	75.0(3)
O(111)−Fe(1)−N(1)	98.1(2)	O(171)−Fe(1)−O(111)	149.6(2)
O(111)−Fe(1)−O(11)	94.8(2)		
O(211)−Fe(2)−N(21)	75.2(3)	O(311)−Fe(2)−O(271)	88.0(2)
O(271)−Fe(2)−N(21)	74.8(3)	O(311)−Fe(2)−N(31)	74.3(3)
O(271)−Fe(2)−O(211)	150.0(2)	O(371)−Fe(2)−N(21)	107.6(2)
N(31)−Fe(2)−N(21)	177.6(3)	O(371)−Fe(2)−O(211)	90.0(2)
N(31)−Fe(2)−O(211)	105.7(2)	O(371)−Fe(2)−O(271)	99.0(2)
N(31)−Fe(2)−O(271)	104.3(2)	O(371)−Fe(2)−N(31)	74.8(3)
O(311)−Fe(2)−N(21)	103.3(2)	O(371)−Fe(2)−O(311)	149.1(2)
O(311)−Fe(2)−O(211)	98.9(2)		

thermodynamic stability ($\log \beta_2 = 17.13$[15a]) with respect to the Fe(II) analogue. It could also explain the kinetic inertia of this species which can be recrystallised in acidic medium without showing any degradation and can also act as a counterion like PF_6^- or BF_4^-.

The two dipic ligands are planar, with deviations from the mean plane smaller than 0.09 Å, except for O(171), which deviates by 0.17 Å. This deviation is probably due to the proximity of the Na^+ cation at a distance of 2.693(3) Å. This cation is also surrounded by six other oxygen atoms: O(72), O(111), O(171), and O(172) and the two water oxygen atoms. The water molecules are also involved in weak intermolecular H-bonds with O(12)−O(100) = 2.944(5) Å, O(12)−H(102) = 2.09(6) Å, O(72)−O(200) = 2.851(5) Å, and O(72)−H(201) = 2.06(5) Å. This dense intermolecular network is probably the cause of the nonlinearity of N(11)−Fe(1)−N(1) (167.4(1)°).

The magnetic moment of the ammonium salt, measured with a Faraday balance, is 6.22 μ_B at 300 K, a value consistent with a high-spin isolated Fe(III). This value decreases very slowly at very low temperature. The long intermolecular Fe−Fe distances (minimum 6.982 Å) and the absence of strong hydrogen bonds preclude any intermolecular interactions but suggest zero-field splitting. Simulation of the variation of the magnetic moment with temperature gave a very good fit (residual 6.22×10^{-5}) with $g = 2.098$ and $|D| = 1.8526$ cm^{-1}.

Implications for the Energy of Intervalence Transitions in Iron(II)−Iron(III) Complexes with Ligands Related to Dipicolinate. The bond length values for the isostructural iron(II) and iron(III) complexes allow us to estimate the wavelengths of the intervalence band in mixed-valence dinuclear complexes $[(dipic)Fe^{II}(dipic-R-dipic)Fe^{III}(dipic)]^{3-}$. The in-

(34) See for example: (a) Long, G. L.; Galeazzi, G.; Russo, U.; Valle, G.; Calogero, S. *Inorg. Chem.* **1983**, *22*, 507. (b) Lintvedt, R. L.; Schoenfelner, B. A.; Ceccarelli, C.; Glick, M. D. *Inorg. Chem.* **1984**, *23*, 2867. (c) Long, G. L.; Clarke, P. J. *Inorg. Chem.* **1978**, *17*, 1394. (d) Haynes, J. S.; Rettig, S. J.; Sams, J. R.; Thompson, R. C.; Trotter, J. *Can. J. Chem.* **1986**, *64*, 429.

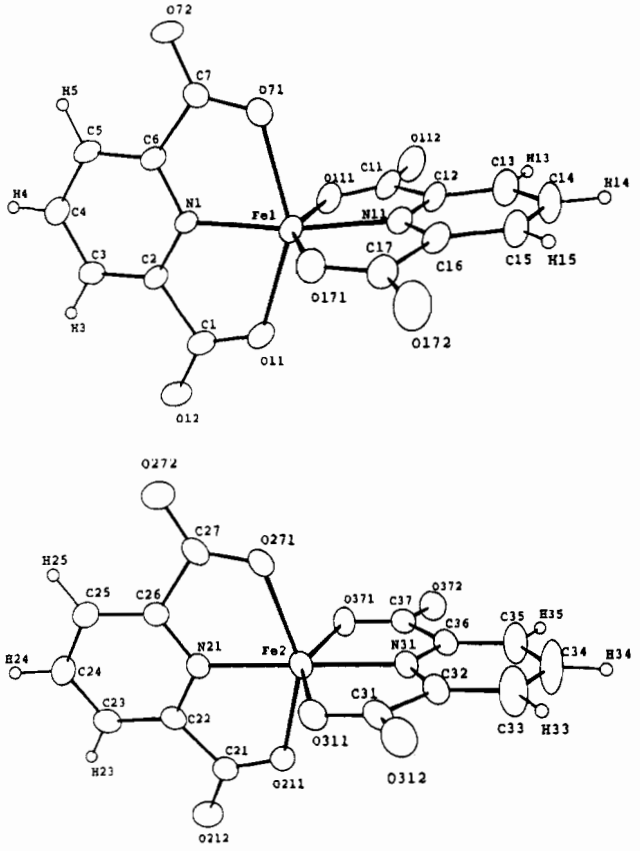

Figure 5. Structures of the $[(dipic)_2Fe^{II}]^{2-}$ anions in **3**, showing atom-labeling schemes.

Table 9. Hydrogen-Bond Distances in **3** (Å)

O(12)−H(702)	1.856(6)	O(12)−O(700)	2.783(8)
O(72)−H(302)	1.888(6)	O(72)−O(300)	2.806(9)
O(112)−H(201)	1.703(7)	O(112)−O(200)	2.797(9)
O(272)−H(701)	1.665(7)	O(272)−O(700)	2.833(9)
O(272)−H(101)	1.783(6)	O(272)−O(100)	2.799(8)
O(372)−H(501)	1.797(6)	O(372)−O(500)	2.777(9)
O(500)−H(402)	1.785(7)	O(500)−O(400)	2.715(9)
O(700)−H(401)	1.850(6)	O(700)−O(400)	2.854(9)

ner-shell energy for optical electron transfer E_{in}^{opt} is given by[35]

$$E_{in}^{opt} = \sum(k_{II} + k_{III})(d_{II} - d_{III})^2/2$$

where d are the bond lengths and k the force constants for oxidation states II and III, the summation bearing on the metal−ligand bonds of one site. The detailed comparison between $[(dipic)_2Fe^{III}]^-$ and $[(dipic)_2Fe^{II}]^{2-}$ shows that the addition of 1 electron to the iron(III) complex increases the Fe−O bonds, but not the Fe−N ones, so that the carboxylate groups move slightly outward (see Figure 7).

Thus we take $Fe^{II}-O = 2.18$ Å, $Fe^{III}-O = 2.03$ Å, $k_{Fe^{II}-O} = 149$ N m^{-1}, and $k_{Fe^{III}-O} = 235$ N m^{-1} [36] and discard the iron−nitrogen bonds. The calculation gives $E_{in} = 17.28 \times 10^{-20}$ J, so that this contribution alone would correspond to a photon of $\lambda = 1150$ nm. However, one has to add the contribution of the outside medium (the solvent) E_{out}^{opt} which can be estimated by the usual Hush−Marcus relation

$$E_{out}^{opt} = [1/(4\pi\epsilon^\circ)](\Delta e)^2(\epsilon_{op}^{-1} - \epsilon_s^{-1})(a^{-1} - R^{-1})$$

where $\Delta e = 1$ e for an optical electron transfer, ϵ_{op} and ϵ_s are the optical and static dielectric constants of the solvent, a is the radius of the coordination sphere (assumed the same for the two oxidation states), and R is the center-to-center distance between sites.[35] Taking for water $\epsilon_{op} = n^2 = 1.77$ and $\epsilon_s = 80$ and for the bis(dipicolinate) (4,4′-bipyridine-2,2′,6,6′-tetracarboxylic acid) complex $a = 5$ Å and $R = 11$ Å, this gives $E_{out}^{opt} = 13.86 \times 10^{-20}$ J, i.e. a value comparable to E_{in}^{opt}. Adding the two contributions to E^{opt} gives finally $\lambda_{intervalence} = ca.$ 640

(35) Brunschwig, B. S.; Logan, J.; Newton, M. D.; Sutin, N. *J. Am. Chem. Soc.* **1980**, *102*, 5798.

Table 10. Selected Atomic Coordinates and Equivalent Isotropic Thermal Parameters (Å^2) for $[(dipic)_2Fe^{III}]Na\cdot 2H_2O$ (**4**)

atom	*x/a*	*y/b*	*z/c*	*U*(iso)[a]
Na(1)	−0.14360(8)	0.1332(1)	0.37616(9)	0.0341
Fe(1)	0.09712(7)	0.24707(5)	0.1253(1)	0.0238
N(1)	0.1283(2)	0.0872(3)	0.1536(4)	0.0236
C(1)	0.2368(3)	0.1557(3)	0.3335(4)	0.0265
C(2)	0.1936(2)	0.0585(3)	0.2573(4)	0.0235
C(3)	0.2123(3)	−0.0487(3)	0.2836(5)	0.0281
C(4)	0.1607(3)	−0.1247(3)	0.2014(5)	0.0298
C(5)	0.0921(3)	−0.0932(3)	0.0950(5)	0.0276
C(6)	0.0784(3)	0.0155(3)	0.0746(4)	0.0231
C(7)	0.0111(2)	0.0710(3)	−0.0363(5)	0.0238
O(11)	0.2011(2)	0.2454(2)	0.2901(3)	0.0322
O(12)	0.3003(2)	0.1456(2)	0.4288(3)	0.0349
O(71)	0.0183(2)	0.1742(2)	−0.0365(3)	0.0281
O(72)	−0.0420(2)	0.0179(2)	−0.1178(3)	0.0327
N(11)	0.0570(2)	0.4039(2)	0.1457(4)	0.0226
C(11)	0.1756(3)	0.4294(3)	−0.0193(5)	0.0271
C(12)	0.1041(2)	0.4791(3)	0.0754(4)	0.0233
C(13)	0.0841(3)	0.5871(3)	0.0929(5)	0.0267
C(14)	0.0137(3)	0.6137(3)	0.1849(5)	0.0307
C(15)	−0.0337(3)	0.5343(3)	0.2569(5)	0.0302
C(16)	−0.0090(2)	0.4287(3)	0.2352(4)	0.0233
C(17)	−0.0467(3)	0.3286(3)	0.3078(5)	0.0259
O(111)	0.1748(2)	0.3257(2)	−0.0191(3)	0.0299
O(112)	0.2277(2)	0.4850(2)	−0.0872(4)	0.0352
O(171)	−0.0013(2)	0.2427(2)	0.2808(3)	0.0287
O(172)	−0.1127(2)	0.3308(2)	0.3829(4)	0.0354

[a] Equivalent isotropic *U*(iso) defined as one-third of the trace of the orthogonalized tensor.

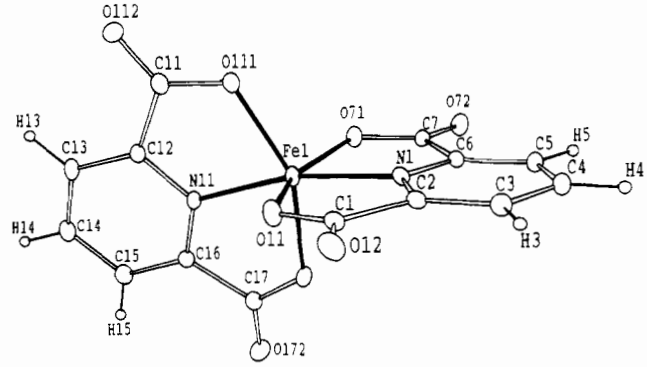

Figure 6. ORTEP drawing of the anion in **4**.

Table 11. Selected Bond Distances (Å) and Angles (deg) for $[(dipic)_2Fe^{III}]Na\cdot 2H_2O$ (**4**)

Fe(1)−N(1)	2.057(3)	C(1)−O(12)	1.230(5)
Fe(1)−O(11)	2.053(3)	C(7)−O(71)	1.290(5)
Fe(1)−O(71)	2.000(3)	C(7)−O(72)	1.227(5)
Fe(1)−N(11)	2.055(3)	C(11)−O(111)	1.293(5)
Fe(1)−O(111)	2.007(3)	C(11)−O(112)	1.217(5)
Fe(1)−O(171)	2.047(3)	C(17)−O(171)	1.296(5)
C(1)−O(11)	1.286(5)	C(17)−O(172)	1.210(5)
O(11)−Fe(1)−N(1)	75.5(1)	O(111)−Fe(1)−O(71)	97.1(1)
O(71)−Fe(1)−N(1)	76.4(1)	O(111)−Fe(1)−N(11)	76.7(1)
O(71)−Fe(1)−O(11)	151.4(1)	O(171)−Fe(1)−N(1)	93.5(1)
N(11)−Fe(1)−N(1)	167.4(1)	O(171)−Fe(1)−O(11)	94.9(1)
N(11)−Fe(1)−O(11)	99.4(1)	O(171)−Fe(1)−O(71)	91.9(1)
N(11)−Fe(1)−O(71)	109.2(1)	O(171)−Fe(1)−N(11)	75.3(1)
O(111)−Fe(1)−N(1)	114.3(1)	O(171)−Fe(1)−O(111)	152.0(1)
O(111)−Fe(1)−O(11)	89.8(1)		

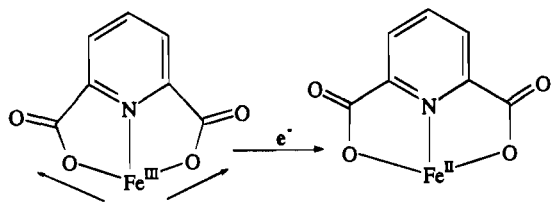

Figure 7. Comparison of the Fe^{II} and Fe^{III} geometries in $[(dipic)_2Fe]$ complexes.

nm. Incidentally, this is not surprising for intervalence transitions involving high-spin iron(II) and iron(III) in oxygen or oxygen–nitrogen environments (cf. $\lambda = 600-700$ nm in several minerals[37] and $\lambda = 740$ nm in a binuclear complex[38]).

Since in the dipic complexes the MLCT band tail is very long, it is very likely that the weak intervalence band will be at least partially masked by the MLCT band at these wavelengths. This is confirmed by the absorption spectrum of the mixed-valence species $[(dipic)Fe^{II}(dipic-dipic)Fe^{III}(dipic)]^{3-}$.[39]

(36) The force constant for iron(II) has been taken from: Basolo, F.; Pearson, R. G. *Mechanisms of Inorganic Reactions*, 2nd ed.; Wiley: New York, 1967; p 458. The force constant for iron(III) was calculated from the previous one using the estimated stretching frequency of $Fe(H_2O)_6^{3+}$ given in ref 35.

(37) Burns, R. G. In *Mixed Valency Systems*; Prassides, K., Ed.; Kluwer: Dordrecht, The Netherlands, 1991; p 175.

(38) Bominaar, E. L.; Ding, X.-Q.; Bill, E.; Winkler, H.; Trautwein, A. X.; Drüeke, S.; Wieghardt, K. In *Mixed Valency Systems;* Prassides, K., Ed.; Kluwer: Dordrecht, The Netherlands, 1991; p 377.

Conclusion

This preliminary study of the chemistry of iron(II) and iron(III) with dipicolinic acid has pointed out four main results: (i) the 1:1 complex of dipicolinate and iron(II) can be synthesized nearly quantitatively; (ii) we have found a new easy and general way to synthesize $[(dipic)_2Fe^{II}](cation)_2$; (iii) the comparison of the structures of the iron(II) and iron(III) complexes reveals the bond length variations induced by the change in oxidation state, from which an estimation of the intervalence band energy for mixed-valence complexes built from iron and dipic is possible; (iv) the $[(dipic)_2Fe^{II}]^{2-}$ anion exhibits some Lewis base character due to the free oxygens of the carboxylate groups. The last point and its structural consequences will be discussed more thoroughly in the following paper.

Acknowledgment. The authors thank J.-P. Tuchagues, G. Lemercier, and A. Mari (LCC-CNRS, Toulouse, France) for helpful discussions and for measurements and simulations of the Mössbauer and magnetic data.

Supporting Information Available: Complete tables of X-ray crystallographic parameters, atom coordinates, thermal parameters, bond lengths, and bond angles for the complexes (41 pages). Ordering information is given on any current masthead page.

IC950101B

(39) Lainé, P. Unpublished results.